PAPER

NJC
www.rsc.org/njc

Insight into metal–phosphorus bonding from analysis of the electronic structure of redox pairs of metal–phosphine complexes†

Tom Leyssens,*[a] Daniel Peeters,[a] A. Guy Orpen[b] and Jeremy N. Harvey*[b]

[a] *Université catholique de Louvain, Laboratoire de Chimie Quantique, Bâtiment Lavoisier, place Louis Pasteur 1, B-1348 Louvain-la-Neuve, Belgium. E-mail: t.leyssens@chim.ucl.ac.be; Fax: +32 10 47 27 07; Tel: +32 10 47 28 19*

[b] *University of Bristol, School of Chemistry, Cantock's Close, Bristol, UK BS8 1TS. E-mail: Jeremy.Harvey@bristol.ac.uk; Fax: +44 117 925 1295; Tel: +44 117 954 6991*

Received (in Montpellier, France) 10th June 2005, Accepted 17th August 2005
First published as an Advance Article on the web 7th September 2005

Density functional theory calculations reproduce the changes in geometry which are observed experimentally upon oxidation of a range of metal phosphine complexes. Removal of one electron from the metal leads to an *increase* in the M–P bond length, along with a decrease in pyramidalization at the phosphorus atom. These changes had previously been used to suggest that π back-bonding from the metal to the P–R σ* antibonding orbitals plays a role even in complexes of simple alkyl- and aryl-phosphines. Similar changes in geometry are found upon one electron oxidation of the simple model species $Cr(CO)_5(PR_3)$ and $Mo(CO)_5(PR_3)$ (R = H or Me). The analogous ammonia complexes instead undergo a decrease of the M–N bond length upon ionization, consistent with stronger σ-bonding upon increasing the charge on the metal atom. Analysis of the electron density in the neutral and cationic species, and of the *change* in density (this is the finite difference Fukui function) also shows evidence of π back-bonding in the neutral species, and much less in the cationic form.

Introduction

Phosphorus(III) compounds such as alkyl- and arylphosphines, phosphites, and phosphamides, are ubiquitous in organometallic and coordination chemistry.[1,2] The electronic structure and hence the reactivity of the metal complexes can be tuned by changing the groups bonded to phosphorus. The traditional model of the phosphorus–metal bond involves σ donation of the ligand lone pair into an empty metal d orbital (or sd hybrid),[3] and π back-bonding from singly- or doubly-occupied metal d orbitals on the metal atom towards appropriate unoccupied ligand orbitals. It was initially thought that the latter were mainly phosphorus 3d orbitals,[4] but more recently it has been recognized that they are instead antibonding P–X σ* orbitals.[5] Accordingly, the nature of the X groups has a strong influence on the importance of back-bonding effects. When X is very electronegative (*e.g.* in PF_3), the P–X bond is highly polarized and the σ* orbital is low in energy and mainly localized on the P atom, favouring back-bonding. Whereas various theoretical and experimental studies clearly show the back-bonding towards PF_3, PCl_3 and $P(OR)_3$ ligands, the quantitative importance of back-bonding with simple alkyl- and aryl-phosphines is harder to judge, with different methods giving a very different account of the importance of this bonding.

Some studies suggest that aryl- and alkyl-phosphines can be classified as very poor π acceptors or even as σ-only ligands. Tolman's electronic parameter is smallest for alkyl- and aryl-phosphines,[6] and a related study of NMR shielding in LNi$(CO)_3$ complexes also shows these ligands to have a high ratio of σ donor to π acceptor character.[7] Based on the strong correlation between the reduction potentials and the carbonyl stretching frequencies of CpFe(CO)(L)(COMe) complexes with various alkyl- and arylphosphines L, it has been argued that the latter are mainly σ-only ligands.[8] Likewise, the redox potentials of $MeCp(CO)_2MnL$ correlate well with the pK_a values of the corresponding trialkyl- and triarylphosphine ligands L, which have been interpreted in a similar way.[9] These observations have been combined with others within the QALE (quantitative analysis of ligand effects) framework to conclude that the π acceptor character of alkyl- and arylphosphines is mostly unimportant.[10]

Other studies however reach very different conclusions. An extended transition state (ETS) energy analysis of $M(CO)_5PX_3$ complexes[11] shows that π-bonding explains 25% of the total M–P bonding interaction. According to a constrained space orbital variation (CSOV) study of $PdP(CH_3)_3$,[12] the back-bonding contribution to the overall metal–ligand interaction is even more important, and only slightly smaller than that of the σ donation. An investigation of the ^{17}O quadruple constants in $WL(CO)_5$ complexes classifies the PMe_3 ligand as a substantially stronger π acceptor than the neutral amine ligand.[13]

With so many divergent conclusions about back-bonding in aryl- and alkylphosphines and very little clear-cut evidence showing that such bonding exists, it is still of interest to examine them to ascertain whether back-bonding does indeed exist.

Some of the most persuasive studies supporting the existence of such bonding effects are based on structural data derived from a survey of a set of metal complex redox pairs,[14,15] in which the change in oxidation state is primarily due to a change in the d electron count at the metal atom. By examining the structures of a range of phosphine complexes which have been

† Electronic supplementary information (ESI) available: B3LYP and BP86 relative energetics of different spin states of the target compounds. Details of experimental and computed bond lengths and angles in reduced and oxidized forms. See http://dx.doi.org/10.1039/b508219f

DOI: 10.1039/b508219f

characterized crystallographically in at least two distinct redox states, it was found that removal of a d electron was correlated with geometrical changes consistent with a decrease in the importance of back-bonding. The most important change is a lengthening of the M–P bond, which is clearly expected if the π interaction is weakened, but is the *opposite* effect from that expected if one considers only the σ framework: increasing the oxidation state of the metal should lead to stronger interaction with the phosphorus lone pair. Indeed, for ligands which clearly interact with the metal only by σ-bonding, such as halides, shortened bonds are observed in the oxidized species.[15]

Smaller but equally significant changes are a shortening of the P–X bonds in the phosphorus ligand, which again is expected due to decreased occupation of the P–X σ* orbitals, and an opening of the X–P–X angles between the substituents on the phosphorus ligand, which corresponds to decreased pyramidalization at the phosphorus centre. The latter effects were rationalized using a qualitative molecular orbital argument based on the Walsh diagram for PX_3 species.[15] In such species, the three σ* orbitals split into a lower-energy degenerate pair of *E* symmetry, and a higher-energy A_1 orbital. The pair of *E* orbitals, which have π symmetry in metal complexes and are thereby responsible for back-bonding, become lower in energy as pyramidalization is increased. Upon metal oxidation, the decrease in back-bonding will remove electrons from these orbitals, so that pyramidalization will decrease. In another structural study of a set of related triphenylphosphine complexes it was observed that, in cases where strong π-bonding was expected to occur, the M–P bonds were shorter, the P–C bonds longer, and the C–P–C angles smaller.[16] This structural argument appears to provide compelling evidence for back-bonding playing a significant role even in alkylphosphines.

However, it is in principle possible that the structural changes have other causes. The most obvious of these is that the nature and number of counterions will change upon changing the oxidation level, although these are not present in the first coordination sphere of the metal in the chosen set of compounds,[15] and that crystal packing effects could also clearly lead to substantial changes in geometry. Also, the structural survey did not provide quantitative insight into the electronic structure of the redox pairs, showing that back-bonding does indeed decrease in these specific examples upon oxidation. It is therefore of interest to confirm whether the observed structural changes can be reproduced using computation (which treats the complexes as isolated gas-phase species), and whether they correlate with the expected bonding changes. The aim of the present study is to examine this question for a range of species which showed evidence of back-bonding in the earlier structural survey. We use a tool from conceptual density functional theory,[17] the Fukui function, to analyze the bonding in the reduced species and the changes in bonding upon oxidation.

Computational details

Geometries of the selected species (see Table 1) were taken from the Cambridge Structural Database[18] in their neutral (reduced) and oxidized (cationic) forms, and any counterions were then deleted to yield the starting points for full DFT geometry optimization. All structures were optimized using Becke's three parameter hybrid functional (B3LYP), as implemented in the Jaguar program.[19] For the central metal atom, an effective core potential was used to represent all but the valence *n*d and (*n* + 1)s and outer core *n*s and *n*p electrons.[20] The latter were described with a triple zeta contraction of the original double zeta basis set; this combination is referred to as the LACV3P basis set. All non-metal atoms were described using the standard 6-31G* basis set (with only the five spherical harmonic d functions). Some additional single-point energies were computed at the B3LYP geometries using the standard BP86 gradient-corrected functional.

Molecular densities, orbital representations, as well as NBO[22] population analysis, were obtained by single-point calculations using the same basis sets, at the Jaguar B3LYP geometries, but using the Gaussian series of programs.[23]

Table 1 Target compounds, with Cambridge Structural Database reference codes [dmpe = $(Me_2P)CH_2CH_2(PMe_2)$, dppe = $(Ph_2P)CH_2CH_2(PPh_2)$, Cp* = $\eta^5C_5Me_5$]

	Neutral/cation
trans-[$MoCl_2$(dmpe)$_2$]	DOWKEF[a]/DOWKIJ[a]
trans-[$CrCl_2$(dmpe)$_2$]	DAJDUN[b]/DOZBEZ[c]
trans-[$TcCl_2$(dppe)$_2$]	JABJAX[d]/JABJEB[d]
[Mn(CO)(dppe)(η^5-C_6H_6Ph)]	DEDPIL[e]/DEDPOR[e]
[FeCp*(C≡C–$C_6H_4NO_2$)(dppe)]	QOZHOC[f]/QOJBAS[f]
[Fe{$P(CH_2CH_2PPh_2)_3$}(C≡C–Ph)]	PEFZAB[g]/PEFYUU[g]
[FeCp*(dppe)]	ZOQJUK[h]/ZOQKAR[h]
[Cp*$MoCl_2(PMe_2Ph)_2$]	YOVGUL[i]/YOVHAS[i]
[η^7-(C_7H_7)Mo(C≡CPh)(dppe)]	KIMSEE[j]/SAZSUH10[j]

[a] Ref. 21*a*. [b] Ref. 21*b*. [c] Ref. 21*c*. [d] Ref. 21*d*. [e] Ref. 21*e*. [f] Ref. 21*f*. [g] Ref. 21*g*. [h] Ref. 21*h*. [i] Ref. 21*a*. [j] Ref. 21*j*.

Results

Structural variations

The species selected for study in this paper are listed in Table 1. We have first checked the correct electronic state for the cationic and neutral species, as in some cases several different spin states are conceivable. We have optimized the geometry of all conceivable spin states for all species (for details, see Table S1 in the ESI†). In most of the cases (except molecules *trans*-[$TcCl_2$(dppe)$_2$], [FeCp*(C≡C–$C_6H_4NO_2$)(dppe)] and [(η^7-C_7H_7)Mo(C≡CPh)(dppe)]), the nature of the ground state is known from experiment, and for most of these the computations agree. However, for *trans*-[$CrCl_2$(dmpe)$_2$] a quintet ground state is predicted, although the (experimentally found) triplet ground state lies very close in energy. It is possible that this discrepancy is due to the neglect of the crystal environment in our calculations. However, it is known that DFT methods can lead to very different spin-state splittings depending on which functional is used, and in particular on the amount of exact exchange included in hybrid functionals.[24] In almost all cases, increasing the proportion of exact exchange lowers the energy of high-spin states. For many cases, there is evidence that B3LYP, with 20% exact exchange, is too strongly biased in favour of high-spin states, with functionals with somewhat less exchange giving better results.[25] It can therefore be expected that in the *trans*-[$CrCl_2$(dmpe)$_2$] case, the correct spin-state, even in the gas phase, corresponds to the intermediate triplet state and that the predicted quintet state is an artefact of the B3LYP method. Indeed, single point BP86 calculations on the different spin states of this compound yield an energy ordering which is compatible with experiment: the triplet lies 16.4 kcal mol^{-1} lower than the quintet. For the cases where no experimental evidence is available, B3LYP predicts low-spin singlet or doublet ground states with large spin-state splittings, and this can safely be assumed to be correct. In the rest of the paper, we consider only the geometry and electronic properties of the experimental or lowest energy spin state.

Some key bond lengths and angles for two selected (but typical) cases are shown in Table 2 (parameters for other species can be found in the ESI†). The agreement between experiment and theory is not excellent in absolute terms, with metal–ligand bond lengths differing by up to 0.07 Å, with the computed value being larger than the experimental. This is in fact not unexpected as it is a fairly common observation that

Table 2 Calculated and experimental bond lengths r(X–Y) (Å) and angles α(X–Y–Z) (°) of neutral *trans*-[$CrCl_2$(dmpe)$_2$] and [FeCp*(dppe)], and changes in these properties upon oxidation to the cationic species

(a) *trans*-[$CrCl_2$(dmpe)$_2$]

	r, α calc.	r, α exp.	Δr, $\Delta\alpha$ calc.	Δr, $\Delta\alpha$ exp.
r(Cr–Cl)[a]	2.402	2.345	−0.074	−0.053
r(Cr–P)[a]	2.444	2.370	0.071	0.076
r(P–Me)[a]	1.851	1.824	−0.010	−0.015
r(P–CH_2)[a]	1.875	1.858	−0.013	−0.037
α(C–P–C)[b]	102.30	100.85	2.50	2.85

(b) [FeCp*(dppe)]

	r, α calc	r, α exp	Δr, $\Delta\alpha$ calc	Δr, $\Delta\alpha$ exp
r(Fe–P)[a]	2.186	2.137	0.130	0.110
r(Fe–Cp*)[c]	1.808	1.722	0.012	0.046
r(P–Ph)[a]	1.859	1.844	−0.026	−0.038
r(P–CH_2)[a]	1.887	1.855	−0.012	−0.025
α(C–P–C)[b]	101.65	100.40	4.39	4.05

[a] Average of the different Cr–Cl, Cr–P, *etc*. bond lengths. [b] Average of the different C–P–C angles. [c] Distance from iron to centroid of cyclopentadienyl ring.

gas phase B3LYP calculations tend to overestimate the length of metal–heteroatom bonds.[11] More important from our point of view is that the change in bond lengths and angles upon removing an electron are well reproduced, to within 0.02 Å or 1°, or better, as also shown in Table 2. Agreement with experiment for these key geometric changes is good for the other systems also (see the ESI†).

We also consider some simple model complexes in which, due to their higher symmetry, π-bonding effects can be more easily discerned. These are the C_s-symmetric $M(CO)_5L$ complexes, with M = Cr or Mo, and L = PH_3, PMe_3 or NH_3, thereby including both 3d and 4d metals as well as ligands to which back-bonding is expected (PH_3 and PMe_3), as well as reference systems in which it should not be observed (NH_3). As for the more complicated species, we consider both reduced (neutral, d^6) and oxidized[26] (cationic, d^5) forms of these model compounds.

For these model complexes, the structural changes upon oxidation are shown in Table 3. For the PH_3 and PMe_3 complexes, these are remarkably similar, and follow the same pattern as found above. The lengthening of the M–P bond, shortening of the P–H or P–C bond, as well as the opening of the H–P–H or C–P–C angle, and the lengthening of the M–C bond and shortening of the C–O bond are all consistent with a decrease in back-bonding towards the PH_3 (or PMe_3) and CO ligands upon ionization. For the complexes of ammonia, the structural changes upon ionization are (except of course for the lengthening and shortening of the M–C and C–O bonds, respectively) *opposite* to those found with the phosphine complex. The main change is a *shortening* of the M–N bond, which can be readily understood as being due to stronger metal–ligand σ interaction for the cationic complex. It can also be noted that the variations in the C–O and M–C bond lengths of the *trans*-CO ligand are more important for the amine complexes than with PH_3 or PMe_3. This suggests that PH_3 and the *trans*-CO ligand compete for back-bonding from the same metal d orbital, thereby weakening the back-bonding to CO. As this competition is no longer present with the NH_3 ligand, stronger CO back-bonding effects are seen for the latter.

Table 3 Changes in bond lengths r(X–Y) (Å) and angles α(X–Y–Z) (°) upon oxidation of neutral model species $M(CO)_5(PX_3)$ to yield cations

	$Cr(CO)_5PH_3$	$Cr(CO)_5PMe_3$	$Cr(CO)_5NH_3$
Δr(Cr–C) *cis*[a]	0.063	0.057	0.068
Δr(C–O) *cis*[a]	−0.014	−0.014	−0.015
Δr(Cr–C) *trans*	0.104	0.102	0.118
Δr(C–O) *trans*	−0.018	−0.018	−0.020
Δr(Cr–P/N)	0.094	0.074	−0.050
Δr(P/N–X)[b]	−0.007	−0.008	0.003
$\Delta\alpha$(X–P/N–X)[c]	3.061	2.040	−1.010
	$Mo(CO)_5PH_3$	$Mo(CO)_5PMe_3$	$Mo(CO)_5NH_3$
Δr(Mo–C) *cis*	0.043	0.040	0.046
Δr(C–O) *cis*	−0.012	−0.012	−0.014
Δr(Mo–C) *trans*	0.082	0.091	0.090
Δr(C–O) *trans*	−0.016	−0.016	−0.018
Δr(Mo–P/N)	0.058	0.047	−0.057
Δr(P/N–X)[b]	−0.006	−0.008	0.004
$\Delta\alpha$(X–P/N–X)[c]	3.086	2.133	−0.993

[a] Average for the four *cis*-CO ligands. [b] Average change for the three P–H, P–C, N–H or N–C bond lengths. [c] Average change of the three X–P(or N)–X angles.

It should be noted that it is difficult to deduce quantitative information concerning the strength of back-bonding from these results. For example, one might expect stronger back-bonding in the molybdenum compounds than in the chromium ones, yet the increase in the Cr–P bond length upon oxidation is greater than the change in the Mo–P bond length. However, it should be noted that the observed changes in bond lengths and angles are the result of a combination of many factors, of which the strength of back-bonding is only one. For example, oxidation also leads to an *increase* in the strength of an M–P σ bond, as observed for the ammonia complexes, which on its own would lead to a shortening of the M–P distance, and this effect may compete more strongly in the Mo case than in the Cr one. Insight into the relative quantitative importance of back-bonding for different complexes and different ligands is therefore not easily available from the structural data reported here.

Density differences

As discussed above, the theoretically obtained geometrical changes match the experimental ones, which gives considerable support to their interpretation in terms of back-bonding[14–16] as crystal packing and counterion effects can be ruled out. A more direct confirmation of the role of back-bonding can be obtained by a bonding analysis. This latter can be done in several ways, *e.g*. by analysing the relevant molecular orbitals. However, as we are treating neutral and cationic species, a natural way of analysing bonding here is by considering the change in electron density upon ionization. The density difference between a reduced (neutral) and oxidized (cationic) species is also the approximate Fukui function shown in eqn (1).

$$f^-(r) = \left[\frac{\partial(\rho(r))}{\partial N}\right]^-_{v(r)} \approx \frac{\rho^0 - \rho^+}{N^0 - N^+} = \rho^0 - \rho^+ \qquad (1)$$

The Fukui function was introduced in the context of density functional theory by Parr and Yang in 1984,[27] and corresponds to the derivative of the electron density with respect to the number of electrons. In practice, this function usually needs to be approximated as a finite-difference term corresponding to removing (f^-) or adding (f^+, not considered here) a whole electron. In a frozen orbital ansatz, these Fukui functions correspond to the density of the HOMO (or, for f^+, of the LUMO), thereby showing their close relation to Fukui's original ideas about frontier MO reactivity.[28]

However, the frozen orbital approach is by no means necessary, and it is possible to compute the density difference whilst taking into consideration the relaxation of all orbitals upon ionization. The Fukui function can thereby be seen to correspond to a "two-step" process: ionization out of the

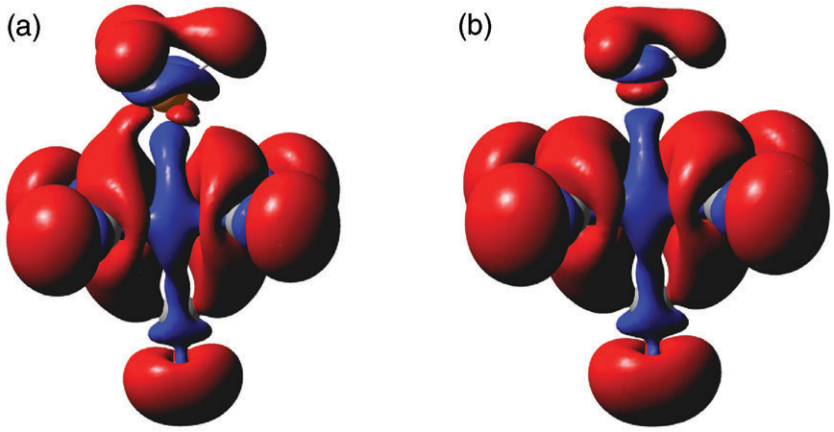

Fig. 1 Fukui functions of (a) $Mo(CO)_5PH_3$ and (b) $Mo(CO)_5NH_3$ taken at an isodensity value of 0.001 e $Bohr^{-3}$.

highest occupied orbital, followed by an electronic redistribution due to the relaxation of all orbitals [eqn. (2)].

$$f^{-}(r) = \rho_{\mathrm{HOMO}} + \rho_{\mathrm{relax}} \qquad (2)$$

By including the latter effect, the Fukui function describes bonding more completely than frontier orbital densities, which are only one of its components. In addition, the finite difference Fukui function is a physical observable, whereas frontier orbitals are only mathematical constructs. Also, Fukui functions are not limited to single determinant electronic structure methods, but can be obtained at any level of theory as long as a total electron density is obtained. These functions are increasingly used to describe electronic structure and reactivity,[17] and in at least one recent example, it has been found that electron relaxation effects can be very important in transition metal chemistry, with frontier orbitals failing to account for experimental observations which are explained using Fukui functions.[29] The present use of the Fukui function to explore bonding properties is, to our knowledge, the first application of this type in transition metal chemistry.

Fig. 1 shows the Fukui function for the $Mo(CO)_5PH_3$ and $Mo(CO)_5NH_3$ complexes.‡ The results for the corresponding chromium complexes are very similar and are not shown. As expected, red zones, corresponding to loss of electron density, predominate. The geometry is such that the Mo–P/N axis is the *z* axis, and the *xz* plane bisects the carbonyl ligands and contains one of the N–H or P–H bonds. Ionization occurs formally out of the metal d_{xz} orbital. The shape of this orbital can be clearly discerned in the centre of both pictures. However, some regions of increased electron density are also found; these regions, shown in blue, are mostly located along the metal–ligand bond, and are due to polarization of the ligand's electron density and hence to the improved metal–ligand σ-bonding in the cationic complexes. In turn, this will lead to some polarization of the P–H and N–H bonds.

Of most interest in the present context are the losses in electron density due to a decrease in back-bonding. These losses are clearly seen on all CO ligands. Despite the fact that ionization occurs from the metal d_{xz} orbital only, the loss in back-bonding is visible all around the CO ligands, showing that the "equatorial" $d_{x^2-y^2}$ orbital also becomes a less effective π donor upon ionization, which is due to the fact that removing an electron lowers the energy of all d orbitals. The main difference between the Fukui functions of Fig. 1a and b occurs near the P/N atoms, along the direction of the P–H and N–H bonds but on the opposite side of the P or N atom. In Fig. 1a, a loss of density is clearly seen in this region corresponding to the π-accepting P–H σ* orbitals of the phosphine ligand. However, in Fig. 1b, no such change is seen in the region of the N–H σ*. This remains true even upon plotting the Fukui function with a lower isodensity value. This marked difference is entirely consistent with the fact that significant back-bonding occurs towards the phosphine ligand in the neutral complexes, but that no such interaction is found with the ammonia ligand.

The Fukui functions for the complexes of Table 1 show similar effects, although in some cases they are difficult to analyze due to the low symmetry and large size of many of these complexes. The Fukui function for *trans*-$[CrCl_2(dmpe)_2]$ is relatively easy to understand, and is shown in Fig. 2. In this case, the complex is oriented such that the Cr–Cl bonds lie along the *z* axis, and the Cr–P bonds lie roughly along the *x* and *y* axes. Ionization occurs in a formal sense out of a d_{xy}-type orbital lying in the CrP_4 plane of the dmpe ligands, and the resulting loss in density corresponding to this orbital is clearly visible. As in the $M(CO)_5(XH_3)$ complexes, there is an *increase* in density along the M–P and M–Cl bonds, due to polarization of the P and Cl lone pairs towards the metal. Associated smaller changes in density occur on the dmpe

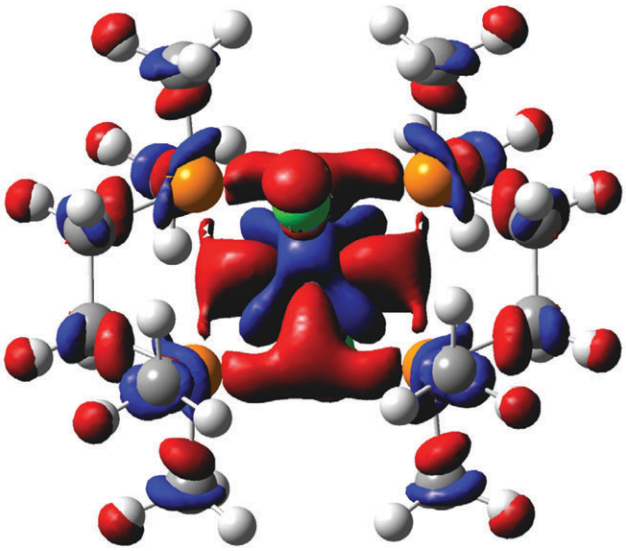

Fig. 2 Fukui function of *trans*-$[CrCl_2(dmpe)_2]$ taken at an isodensity value of 0.002 e $Bohr^{-3}$.

‡ The neutral model complexes have nearly degenerate HOMO and HOMO − 1 orbitals, respectively of *a′* and *a″* symmetry. The cationic complexes treated in this paper are derived from ionization of an electron from the *a′* orbital ($^2A'$ state). There is a very close-lying state (the difference in energy is of the order of 0.1 kcal mol^{-1}), which is derived from ionization from the *a′* orbital ($^2A''$ state). The geometry changes upon ionization to this state are very similar to those discussed in the text for the $^2A'$ state. Note also that the Fukui functions discussed in this paper are derived at the structure of the neutral complex. The corresponding functions computed at the equilibrium structure of the cations are very similar.

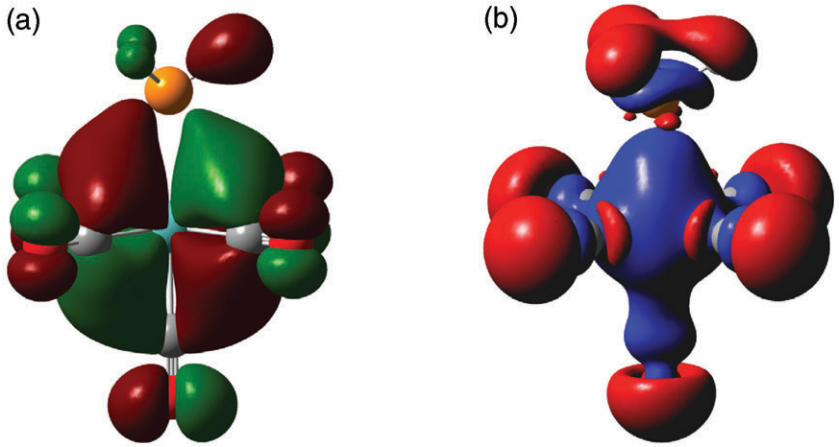

Fig. 3 (a) HOMO (0.02 $e^{1/2}$ $Bohr^{-3/2}$) and (b) relaxation density (0.001 e $Bohr^{-3}$) of $Mo(CO)_5PH_3$.

ligands (and the chlorine ligands) due to this polarization effect. The loss in back-bonding towards the σ* P–C bonds of the dmpe ligands is very clearly visible, with a marked extension of the lobes corresponding to the density loss from the d orbital on the metal towards the regions behind each of the in-plane P–C bonds.

A more detailed analysis of the Fukui function for the simple complexes yields additional insight into the back-bonding. Fig. 3 shows the two components of the Fukui function corresponding to ionization of $Mo(CO)_5PH_3$ [here again, results for $Cr(CO)_5PH_3$ are very similar and are not shown]. The first contribution comes from the loss of density resulting from removing an electron from the HOMO (shown in Fig. 3a), with the second contribution, due to the change in density upon orbital relaxation ρ_{relax} [eqn (2)], shown in Fig. 3b. The HOMO (Fig. 3a) is clearly mainly the metal d_{xz} orbital, although it does show some delocalization onto the CO orbitals and some evidence of back-bonding to the phosphine. However, symmetry restrictions mean that only some of the back-bonding interactions are visible in this plot of the HOMO: contributions from the $d_{x^2-y^2}$ orbital interacting with the CO π* orbitals lying in the equatorial plane, for example, are completely missing. Also, back-bonding appears to occur only towards one of the degenerate combinations of P–H σ* orbitals of *E* symmetry. Fig. 3b shows the relaxation density, which introduces all the effects which are visible in Fig. 1a yet absent in Fig. 3a. The main such effect is the polarization of the metal–ligand bonds, leading to an increase in density around the metal. However, changes relating to back-bonding are also observed, which are due to the decrease in electron-donating character of all the d orbitals upon removing an electron from the metal centre. Small red lobes corresponding to a decrease in back-bonding in the equatorial plane can be seen in Fig. 3b, as well as lobes in the region corresponding to the P–H σ* orbitals. Note that these lobes are larger for the two P–H bonds for which the HOMO density is smaller in Fig. 3a; the sum of the effects is that the overall loss of electron density in Fig. 1, corresponding to back-bonding to each of the P–H antibonding orbitals, is roughly the same.

To obtain quantitative insight into the changes in electron density upon ionization, it is necessary to integrate the Fukui function. In principle, given the presence of basins of increased and decreased electron density, it would be possible to carry out such an integration so as to differentiate between σ and π effects. We have however used NBO population analysis to apportion the total electron density between atoms in the neutral, cationic, and unrelaxed cationic systems. This leads to the condensed Fukui function,[30] the HOMO atomic population, and the condensed relaxation density, as shown in Table 4. The relaxation density was obtained by taking the difference in atomic populations for the relaxed cationic wavefunction and for the cationic wavefunction expanded using the neutral orbitals.

First of all, it can be noted that the density analysis shows that the changes upon ionization are very similar for the chromium and molybdenum complexes, confirming that no major change in the importance of back-bonding or other effects occurs between the 3d and the 4d species. Next, and

Table 4 Condensed Fukui function, HOMO atomic population, and condensed relaxation density for model complexes and *trans*-$[CrCl_2(dmpe)_2]$

$M(CO)_5XH_3$		M = Cr/X = P	M = Mo/X = P	M = Cr/X = N	M = Mo/X = N
Condensed Fukui function	M	0.508	0.530	0.510	0.519
	cis-CO	0.076	0.075	0.085	0.085
	trans-CO	0.088	0.087	0.109	0.106
	PH_3/NH_3	0.099	0.085	0.041	0.036
HOMO atomic population	M	0.818	0.799	0.816	0.785
	cis-CO	0.024	0.025	0.025	0.029
	trans-CO	0.073	0.083	0.083	0.097
	PH_3/NH_3	0.013	0.016	0.001	0.003
Condensed relaxation density	M	−0.309	−0.270	−0.306	−0.265
	cis-CO	0.052	0.049	0.060	0.056
	trans-CO	0.015	0.005	0.026	0.009
	PH_3/NH_3	0.085	0.068	0.040	0.034
trans-[$CrCl_2$(dmpe)2]			Condensed Fukui function	HOMO population	Condensed relaxation density
	Cr		0.411	0.949	−0.538
	Cl		0.065	−0.009	0.074
	dmpe		0.229	0.035	0.195

as expected for a process involving formal metal oxidation, the condensed Fukui function for all species is mainly localized on the metal. However, only *ca.* 50% of the density change upon ionization is located on the metal atom; the sum of the condensed Fukui function on all the other atoms accounts for the other 50%. In particular, for the "back-bonding" ligands (CO and PH_3), ionization leads to a loss in electron density corresponding in total to *ca.* 0.08 electron on each ligand. This loss is due to both a decrease in π back-bonding and an increase in σ electron donation to the central metal atom. The magnitude of the latter effect can be roughly estimated by considering the condensed Fukui function on the ammonia ligand, which is significantly smaller, corresponding to 0.041 and 0.036 electrons, respectively, for the Cr and Mo complexes. However, this σ contribution may of course vary from one ligand to another, so that it is not possible to conclude that π back-bonding is equal in importance for PH_3 and CO ligands despite the similar condensed Fukui functions. It should also be considered that the cationic species retain five d electrons, so that back-bonding will not be completely removed upon ionization.

The change in atomic population is greatest for the *trans*-CO ligand, especially in the presence of the NH_3 ligand. This confirms the picture emerging from the structural changes discussed earlier, whereby there is competitive back-bonding between the *trans*-CO and PH_3 ligands, but not between the *trans*-CO and NH_3 ligands.

It is interesting to consider also the contributions of the atomic HOMO and condensed relaxation densities. Upon considering only the contribution from the HOMO, it might be concluded that ionization is overwhelmingly (*ca.* 80%) metal-centred. The contribution from the PH_3 ligand, in particular, is very small and not much larger than that on the NH_3 ligand. This however neglects the important contribution from the relaxation density, which leads to the further removal of *ca.* 0.07 electrons from the phosphine ligand, due to σ polarization and loss of back-bonding. The relaxation density contribution on the ligand is again much greater than that on NH_3, suggesting that the role of back-bonding for PH_3 is fairly large.

We have also evaluated the condensed Fukui function and its two components for *trans*-[$CrCl_2(dmpe)_2$]. Here too, the HOMO density is mainly on the metal centre, with as much as 0.95 electrons predicted to be removed from the metal upon ionization. However, the relaxation function in this case has an even more drastic effect, such that the condensed Fukui function shows the removal of only 0.4 of an electron from chromium upon ionization. Interestingly, only a small part of the remaining density change is located on the formally anionic chloride ligands (0.065 electrons on each), with a much larger 0.229 electrons coming from each of the dmpe ligands. It is not easy in this case to quantify the contributions from σ polarization effects and decreased back-bonding, but it is likely that both effects play a significant role.

Conclusions

Metal–phosphine bonding in simple PH_3, trialkylphosphine, and triarylphosphine complexes is shown to have a significant π back-bonding component. This is shown in two different ways. First, computed gas phase changes in geometry upon ionization of a range of metal complexes match those identified earlier[14,15] for the same species in a survey of crystalline structures. This shows that crystal packing and counterion effects cannot explain these changes in geometry upon one-electron oxidation, such as the unexpected *lengthening* of the metal–phosphorus bonds. All of these effects can instead be explained by a loss in back-bonding upon ionization.

In order to analyze the electronic structure of the reduced and oxidized species, we use a method which has not been applied before in analysing bonding of transition metal compounds, namely the analysis of the calculated electron densities and the change in density upon ionization (the finite difference Fukui function). This gives valuable qualitative (but not quantitative) insight into the nature of bonding. Plotting the Fukui function confirms that ionization is accompanied by a significant loss in back-bonding to the phosphine P–R σ* orbitals. Similar calculations for ammonia complexes show no evidence of back-bonding. The Fukui function is an accurate description of the changes in bonding upon ionization. In contrast, the HOMO density is much less informative, as it does not include the important orbital relaxation effects.

Acknowledgements

The authors are indebted to the Belgian National Fund for Scientific Research (F.N.R.S.) for its financial support to this research (Tom Leyssens is Research Fellow grant FC 64894). They would like also to thank the F.N.R.S. for its support to access computational facilities (FRFC project N°2.4556.99 "Simulations numériques et traitement des données"). JNH thanks the EPSRC for an Advanced Research Fellowship.

References

1 J. P. Collman, L. C. Hegedus, J. R. Norton, R. G. Finke, *Principles and Applications of Organotransition Metal Chemistry*, University Science Books, Mill Valley, CA, 1987.
2 R. H. Crabtree, *The Organometallic Chemistry of the Transition Metals*, Wiley, New York, 1988.
3 See *e.g.*: J. N. Harvey, K. M. Heslop, A. G. Orpen and P. G. Pringle, *Chem. Commun.*, 2003, 278.
4 (*a*) J. Chatt and A. A. Williams, *J. Chem. Soc.*, 1951, 3061; (*b*) J. Chatt and A. A. Williams, *J. Chem. Soc.*, 1952, 273.
5 (*a*) S. X. Xiao, W. C. Trogler, D. E. Ellis and Z. Berkovitch-Yellin, *J. Am. Chem. Soc.*, 1983, **105**, 7033; (*b*) D. S. Marynick, *J. Am. Chem. Soc.*, 1984, **106**, 4064; (*c*) J. A. Tossell, J. H. Moore and J. C. Giordan, *Inorg. Chem.*, 1985, **24**, 1100.
6 C. A. Tolman, *J. Am. Chem. Soc.*, 1970, **92**, 2953.
7 G. M. Bodner, M. P. May and L. E. McKinney, *Inorg. Chem.*, 1980, **19**, 1951.
8 M. M. Rahman, H. Y. Liu, K. Eriks, A. Prock and W. P. Giering, *Organometallics*, 1989, **8**, 1.
9 M. N. Golovin, M. M. Rahman, J. E. Belmonte and W. P. Giering, *Organometallics*, 1985, **4**, 1981.
10 (*a*) M. M. Rahman, H. Y. Liu, A. Prock and W. P. Giering, *Organometallics*, 1987, **6**, 650; (*b*) H. Y. Liu, K. Eriks, A. Prock and W. P. Giering, *Organometallics*, 1990, **9**, 1758; (*c*) K. Eriks, W. P. Giering, H. Y. Liu and A. Prock, *Inorg. Chem.*, 1989, **28**, 1759; (*d*) A. L. Fernandez, M. R. Wilson, A. Prock and W. P. Giering, *Organometallics*, 2001, **20**, 3429.
11 G. Frenking, K. Wichmann, N. Fröhlich, J. Grobe, W. Golla, D. Le Van, B. Krebs and M. Läge, *Organometallics*, 2002, **21**, 2921.
12 G. Pacchioni and P. S. Bagus, *Inorg. Chem.*, 1992, **31**, 4391.
13 S. P. Wang, M. G. Richmond and M. Schwartz, *J. Am. Chem. Soc.*, 1992, **114**, 7595.
14 A. G. Orpen and N. G. Connelly, *J. Chem. Soc., Chem. Commun.*, 1985, 1310.
15 A. G. Orpen and N. G. Connelly, *Organometallics*, 1990, **9**, 1206.
16 (*a*) B. J. Dunne, R. B. Morris and A. G. Orpen, *J. Chem. Soc., Dalton Trans.*, 1991, 653; (*b*) S. E. Garner and A. G. Orpen, *J. Chem. Soc., Dalton Trans.*, 1993, 533.
17 P. Geerlings, F. De Proft and W. Langenaeker, *Chem. Rev.*, 2003, **103**, 1793.
18 F. H. Allen, *Acta Crystallogr., Sect. B: Struct. Sci.*, 2002, **B58**, 380.
19 Jaguar 5.0, Schrödinger, LLC, Portland, OR, 2002.
20 P. J. Hay and W. R. Wadt, *J. Chem. Phys.*, 1985, **82**, 270.
21 (*a*) L. K. Fong, J. R. Fox, B. M. Foxman and N. J. Looper, *Inorg. Chem.*, 1986, **25**, 1880; (*b*) G.S. Girolami, G. Wilkinson, A. M. R. Galas, M. Thornton-Pett and M. B. Hursthouse, *J. Chem. Soc., Dalton Trans.*, 1985, 1339; (*c*) J. E. Salt, G. Wilkinson, M. Molevalli and M. B. Hursthouse, *J. Chem. Soc., Dalton Trans.*, 1986, 1141; (*d*) K. Libson, M. N. Doyle, R. W. Thomas, T. Welesnik, M. Woods, J. C. Sullivan, R. C. Elder and E. Deutsch, *Inorg. Chem.*, 1988, **27**, 3614; (*e*) N. G. Connelly, M. J. Freeman, A. G. Orpen, A. R. Sheehan, J. B. Sheridan and A. Sivergat, *J. Chem. Soc., Dalton Trans.*, 1985, 1019; (*f*) R. Denis, L. Toupet, F. Paul and C. Lapint, *Organometallics*, 2000, **19**, 4240; (*g*) C.

Bianchini, F. Laschi, D. Masi, F. M. Ottaviani, A. Pastor, M. Peruzzini, P. Zanello and F. Zanokini, *J. Am. Chem. Soc.*, 1993, **115**, 2723; (*h*) P. Hamon, L. Toupet and C. Lapinte, *Organometallics*, 1996, **15**, 10; (*i*) F. Abugideiri, W. D. Keogh, H. B. Kraatz, W. Pearson and R. Poli, *J. Organomet. Chem.*, 1995, **488**, 29; (*j*) R. L. Beddoes, C. Bitron and M. W. Whiteley, *J. Organomet. Chem.*, 1991, **402**, 85–96.

22 A. E. Reed, F. Weinhold and F. Curtiss, *J. Chem. Phys.*, 1985, **83**, 1736.

23 M. J. Frisch, G. W. Trucks, H. B. Schlegel, G. E. Scuseria, M. A. Robb, J. R. Cheeseman, J. A. Montgomery Jr., T. Vreven, K. N. Kudin, J. C. Burant, J. M. Millam, S. S. Iyengar, J. Tomasi, V. Barone, B. Mennucci, M. Cossi, G. Scalmani, N. Rega, G. A. Petersson, H. Nakatsuji, M. Hada, M. Ehara, K. Toyota, R. Fukuda, J. Hasegawa, M. Ishida, T. Nakajima, Y. Honda, O. Kitao, H. Nakai, M. Klene, X. Li, J. E. Knox, H. P. Hratchian, J. B. Cross, C. Adamo, J. Jaramillo, R. Gomperts, R. E. Stratmann, O. Yazyev, A. J. Austin, R. Cammi, C. Pomelli, J. W. Ochterski, P. Y. Ayala, K. Morokuma, G. A. Voth, P. Salvador, J. J. Dannenberg, V. G. Zakrzewski, S. Dapprich, A. D. Daniels, M. C. Strain, O. Farkas, D. K. Malick, A. D. Rabuck, K. Raghavachari, J. B. Foresman, J. V. Ortiz, Q. Cui, A. G. Baboul, S. Clifford, J. Cioslowski, B. B. Stefanov, G. Liu, A. Liashenko, P. Piskorz, I. Komaromi, R. L. Martin, D. J. Fox, T. Keith, M. A. Al-Laham, C. Y. Peng, A. Nanayakkara, M. Challacombe, P. M. W. Gill, B. Johnson, W. Chen, M. W. Wong, C. Gonzalez, and J. A. Pople, *GAUSSIAN 03 (RevisionB.05)*, Gaussian Inc., Pittsburgh PA, 2003.

24 J. N. Harvey, *Struct. Bonding*, 2004, **112**, 151.

25 (*a*) M. Reiher, O. Salomon and B. A. Hess, *Theor. Chem. Acc.*, 2001, **107**, 48; (*b*) O. Salomon, M. Reiher and B. A. Hess, *J. Chem. Phys.*, 2002, **117**, 4729.

26 In the neutral complexes, the HOMO and HOMO − 1 orbitals, respectively of a' and a'' symmetry, are very close in energy. There are therefore two nearly degenerate states of the oxidized species. Our calculations consider the species generated upon ionization from the a' orbital. A nearly degenerate cationic complex (differences of about 0.2 kcal mol^{-1}) having similar structural variations, is found when the ionization occurs out of the a'' orbital.

27 R. G. Parr and W. Yang, *J. Am. Chem. Soc.*, 1984, **106**, 4049.

28 K. Fukui, Y. Yonezawa and H. Shingu, *J. Chem. Phys.*, 1952, **20**, 722.

29 L. J. Bartolotti and P. W. Ayers, *J. Phys. Chem. A*, 2005, **109**, 1146.

30 W. Yang and W. J. Mortier, *J. Am. Chem. Soc.*, 1986, **108**, 5708–5711.